European Rotorcraft Forum

A QUASI-LINEAR PARAMETER VARYING (QLPV) MODELING APPROACH FOR REAL TIME PILOTED SIMULATION OF TILTROTOR

Hafiz Noor Nabi[1,2] and Giuseppe Quaranta[1]

[1]Politecnico di Milano (Italy)
{hafiznoor.nabi, giuseppe.quaranta}@polimi.it

[2]Delft University of Technology (The Netherlands)
h.n.nabi@tudelft.nl

Abstract
Tiltrotors can transform from helicopter configuration to a fixed wing airplane configuration. This allows them to have a broader flight envelope. The dynamics of tiltrotors change with flight condition and aircraft configuration. Therefore, a model stitching technique based on quasi-Linear Parameter Varying (qLPV) framework is employed to develop a continuous full flight envelope flight dynamics model for the purpose of control system design and real time piloted simulation. A high order qLPV model is developed for XV-15 where discrete linear state-space models are *stitched* together to provide a varying model dynamics and trim characteristics over the complete flight envelope. The model is also coupled with engine dynamics, rotor speed governor, actuator dynamics and stability and control augmentation system (SCAS). Lastly, the qLPV model is implemented in FRAME-Sim, a fixed base rotorcraft flight simulation system.

NOMENCLATURE

$\mathbf{A}$	State matrix
$\mathbf{B}$	Control matrix
h	Altitude
V	Velocity
$\mathbf{u_{trim}}$, $\mathbf{x_{trim}}$	Trim control inputs and states
β_{Gs}, β_{Gc}	Lateral and longitudinal rotor gimbal
β_i	Nacelle incidence angle
$\boldsymbol{\rho}(t)$	Scheduling parameter vector
δ_f	Wing flap angle
Ω	Rotor speed
τ_{act}	Actuator time constant
θ	Aircraft pitch angle
$\theta_0, \theta_{1s}, \theta_{1c}$	Collective pitch, longitudinal and lateral cyclic
θ_{gov}	Rotor collective governor

1. INTRODUCTION

Tiltrotors have the ability to fly like a fixed wing airplane at higher cruise speed, range and altitude while keeping the possibility to fly helicopter's S/VTOL tasks. This allows to have a broader flight envelope compared to the flight envelope of conventional and compound helicopters, Figure 1[1]. This advantage of broad flight envelope shows that the tiltrotors represent a good solution to future civil transportation requirements[2,3].

To improve design of future tiltrotor aircraft for civil transportation systems, handling qualities need to be addressed at early design phase. Handling qualities of aircraft are hardly quantifiable and therefore, real time piloted simulations are key to assess the handling qualities through pilot feedback. At the core of such piloted simulations lie a high fidelity flight dynamics model.

The three distinct modes of flight in tiltrotor (helicopter, conversion and airplane) make it particularly challenging to develop continuous full flight envelope models for piloted simulations. The dynamics of a tiltrotor aircraft do not only change with the

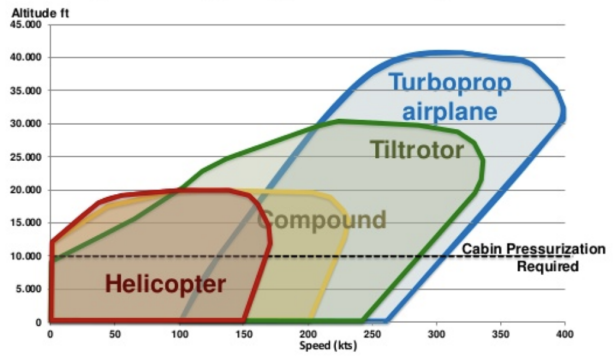

Figure 1: Tiltrotor operating flight envelope advantage[1].

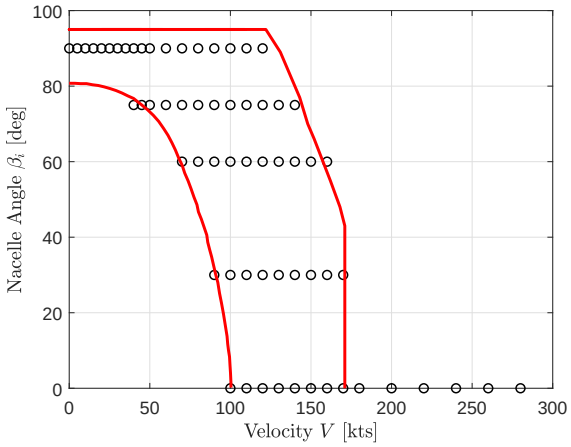

Figure 2: XV-15 linear state-space models and conversion corridor.

flight condition but also with the aircraft configuration, and hence it is fitting to employ stitching technique[4] to model the flight dynamics of a tiltrotor for the purpose of control system design and full flight envelope piloted simulations. The model stitching technique is an extension to quasi-Linear Parameter Varying models[5]. The usage of qLPV *stitched* models for tiltrotor offline simulation and control synthesis has been already proposed by Lawrence et al.[6] for the simulation of NASA's LCTR2 (Large Civil Tiltrotor, 2nd generation) within a limited flight envelope in helicopter mode and by Berger et al.[7] to support the control synthesis of a generic tiltrotor aircraft. In both cases, the linear state-space models were dependant on two scheduling parameters: velocity V and nacelle incidence angle β_i. Additionally, only a limited number of rotor elastic degrees of freedom were used, neglecting the wing elasticity that may play an important role in Rotorcraft Pilot Coupling events[8]. Recently, a qLPV model for XV-15 was developed using a four dimensional scheduling vector of parameters: altitude h, nacelle angle β_i, wing flap angle δ_f and velocity V for conversion maneuver optimization[9]. This qLPV model did not include engine-governor dynamics and hence lacked throttle input.

In the current study, engine-governor dynamics is added to the qLPV stitched model scheduled with four dimensional parameter vector $\rho = \begin{bmatrix} h & \beta_i & \delta_f & V \end{bmatrix}$. The qLPV model is used in real-time in the FRAME-Sim rotorcraft flight simulation, currently being developed at the Department of Aerospace Science and Technology, Politecnico di Milano.

The paper is organized as follows: first the linear state-space models and corresponding trim data are presented. Second, the development of qLPV model is described in detail. Next, the rotorcraft flight simulator FRAME-Sim is detailed. Lastly, a brief conclusion and plans for future research are presented.

2. STATE-SPACE POINT MODELS

Simulation tool MASST (Modern Aeroservoelastic State Space Tools), developed at Politecnico di Milano[10,11], is used to generate a set of aeroelastic linear state-space models and trim data. Rotor aeroelastic models in MASST are obtained from CAMRAD/JA[12] using data published by Acree[13] for XV-15 research aircraft with advanced technology blades (ATBs). The flexible airframe is included using aeroelastic NASTRAN model.

Linear state-space models and trim data (states and control inputs) are obtained at the discrete points that span the entire conversion corridor, Figure 2. Furthermore, each model is also obtained at four wing flap positions ($\delta_f = \begin{bmatrix} 0 & 20 & 40 & 75 \end{bmatrix}$ deg.) and at two altitudes ($h = \begin{bmatrix} 0 & 10000 \end{bmatrix}$ ft.) to obtain a four dimensional grid of linear state-space models and trim data.

2.1. State-Space Formulation

The state-space models contain 91 states comprised of:

- Rigid body states (9)
- Wing bending 1st mode (2)
- Three blade bending modes in multi-blade coordinates (one collective and two cyclic) for each rotor (36)
- Two blade torsional modes in multi-blade coordinates (one collective and two cyclic) for each rotor (24)

- Two gimbal states in multi-blade coordinates (two cyclic) for each rotor (8)
- Three inflow states (average, cosine and sine) for each rotor, based on the classical Pitt Peters model[14] (6)
- Engine dynamics: Rotor speed, differential rotor speed and engine speed perturbation and their integral (azimuth perturbation) (6).

And has 11 inputs:

- Collective pitch θ_0 for each rotor (2)
- Lateral and longitudinal cyclic pitch (θ_{1c}, θ_{1s}) for each rotor (4)
- Aerodynamic control surface deflections (δ_f, δ_e, δ_r, δ_a) (4)
- Engine throttle δ_t (1).

The model has a very high fidelity of the flight mechanics bandwidth and a reasonable representation of the elements that give the most significant contribution to structural loads. It is sufficiently detailed to be used for design and verification of control systems and for the prediction of potential RPC problems[8].

2.2. Trim Data

The linear state-space models are obtained though the linearization and time-invariant approximation of nonlinear time-periodic CAMRAD/JA model[10,12] at assigned trim flight conditions.

The trim flight conditions are composed of selected points, placed regularly on 4-dimensional parameter space $[h \times \beta_i \times \delta_f \times V]$. The rotor rpm is scheduled with speed of the aircraft. At higher speeds ($V \geq 200$ kts), the rotor RPM is reduced from 601 to 480.8.

Trim states and controls at sea level and fixed wing flap angles ($\delta_f = 40^\circ$ for $\beta_i = 90^\circ, 75^\circ$, $\delta_f = 20^\circ$ for $\beta_i = 60^\circ, 30^\circ$ and $\delta_f = 0^\circ$ for $\beta_i = 0^\circ$) are shown in Figure 3, including longitudinal controls (left plot), aircraft pitch attitude, and longitudinal and lateral rotor gimbal (right plot). As expected, trim collective θ_0 and longitudinal cyclic θ_{1s} at high nacelle angles ($\beta_i \geq 75^\circ$) follow a trend similar to that of a conventional helicopter. Below minimum power required speed, trim collective decreases with airspeed, and above it, it starts to increase with airspeed to overcome drag. Furthermore, at low nacelle angles, the trim collective contributes towards the generation of thrust required to keep the increasing forward speed of the aircraft constant.

Trim Longitudinal cyclic θ_{1s} move backwards to compensate for decreasing pitch attitude of the aircraft (top-right plot) at all nacelle angles. Symmetric longitudinal cyclic is used to trim the aircraft for $\beta_i > 0$ and is phased out in airplane mode. Similarly, elevator deflection δ_e decreases (trailing edge up) with increasing speed to trim the increasingly pitch down attitude of the aircraft.

Trim pitch attitude θ decreases with increasing speed for all the nacelle angles. However, at a given speed, the pitch attitude increases with decreasing nacelle incidence angle because more lift is generated by the wings than the rotors in these configurations. Furthermore, at lower nacelle angles (specially in airplane mode $\beta_i = 0^\circ$), the slope of pitch attitude flattens out with speed. Lastly, Figure 3 also show the trim longitudinal and lateral gimbal angles.

2.3. Rotor Speed Governor

A rotor speed governor is implemented to maintain a constant rotor angular speed. The beta-governor[15], shown in Figure 4, is a proportional-integral (PI) controller, Eq. 1, that operates on the feedback of rotor speed error (in rad/sec) and outputs the desired changes of the blade collective pitch to maintain a desired rotor speed. Proportional and integral gains are scheduled with nacelle angle and are listed in Table 1. In helicopter mode, the governor collective pitch input is added to collective pitch coming from pilot stick. As the aircraft changes from helicopter to airplane mode, collective pitch from stick input is phased out.

$$\theta_{\text{gov}} = K_i \int (\Omega - \Omega_{\text{ref}})\, dt + K_p\, (\Omega - \Omega_{\text{ref}}) \tag{1}$$

Table 1: Governor PI gains.

Nacelle angle β_i [deg.]	Kp	Ki
90	0.0524	0.1
75	0.0436	0.1
60	0.0439	0.1
30	0.0174	0.1
0	0	0.1, $V \leq 180$ kts 0.5, $V > 180$ kts

It is observed that the engine dynamics coupled with governor dynamics affects the longitudinal phugoid mode of the aircraft. Figure 5 shows the longitudinal phugoid mode damping for various aircraft configurations as function of aircraft speed at

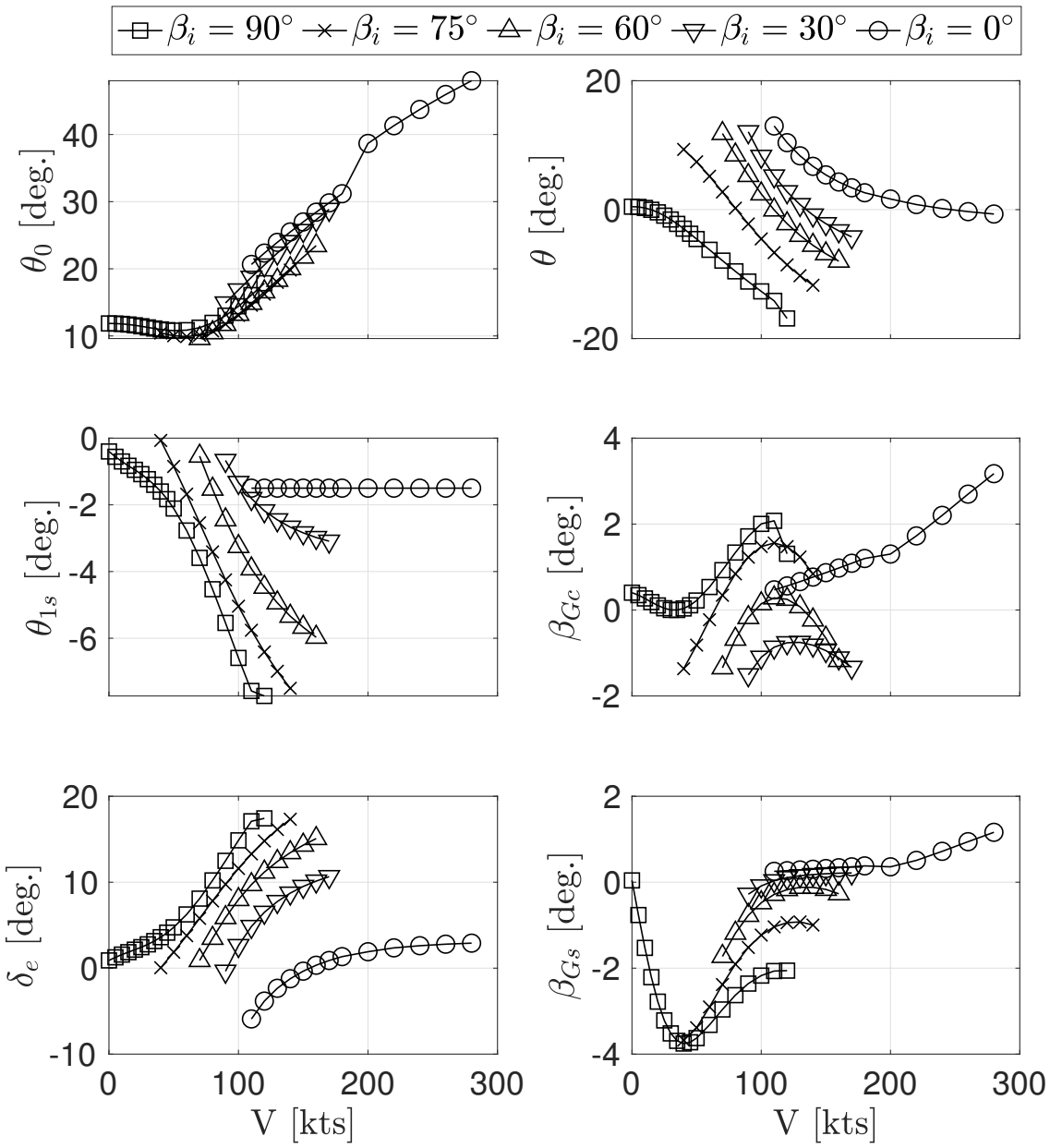

Figure 3: Trim longitudinal control inputs, pitch attitude and rotor gimbal, at sea level and assigned flap angles.

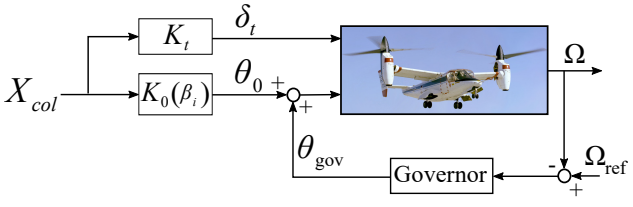

Figure 4: *Beta*-governor block diagram.

different governor integral gains. Additionally, longitudinal phugoid damping for model without engine dynamics (i.e., with constant rotor speed Ω) is also shown in Figure 5. In helicopter mode, the damping increases with the addition of engine dynamics and the governor. However, at lower nacelle angles, phugoid damping decreases when engine dynamics coupled with governor is added to the model. Moreover, the damping increases with speed at high nacelle angles both with and without engine dynamics. At a given nacelle angle, the governor integral gain must be bounded between a minimum and a maximum value with respect to velocity, otherwise the longitudinal phugoid will become unstable. For

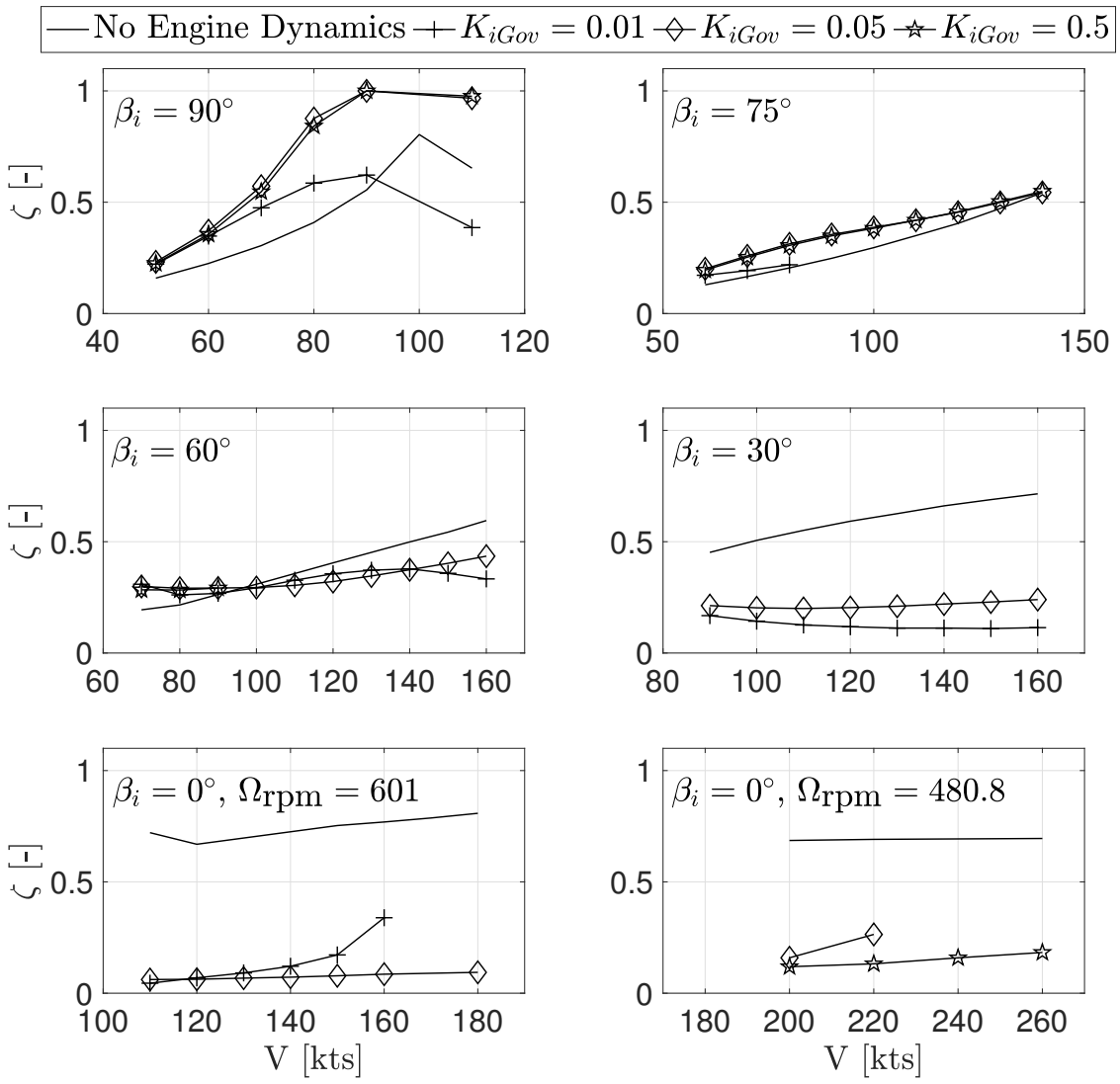

Figure 5: XV-15 Longitudinal phugoid damping (SCAS off).

example, at $\beta_i = 75°$ phugoid mode is unstable for $K_i = 0.01$ at speeds above 80 knots. For $\beta_i = 60°$ and $\beta_i = 30°$, the aircraft is unstable at all the velocities for $K_i = 0.5$. Lastly, in airplane mode $\beta_i = 0°$, the phugoid mode is unstable for high K_i at lowers speeds ($V < 200$ kts) and for low K_i at higher speeds.

2.4. Eigenvalues

Rigid body eigenmodes of linear state-space model of XV-15 obtained from MASST are presented in Table 2. Results of MASST models with and without engine-governor dynamics are listed in the table. In addition, eigenvalues are compared with the data obtained from various references. These reference models include a flightlab model of XV-15[16], a mathematical model of the Bell Model 301 tiltrotor research aircraft[17] and a model obtained form XV-15 flight data using frequency based system identification approach[18]. Overall the comparison is reasonable with published data. Some observations on the comparison are presented in the following paragraphs.

In helicopter mode during hover, XV-15 MASST models with and without engine dynamics are identical. A reasonable match between the eigenvalues of MASST model and Flightlab model is observed. However, the identified model[18] from flight data show higher frequencies in pitch-heave subsidence, longitudinal phugoid and dutch roll mode. At $V = 120$ kts in helicopter mode, the eigenmodes of MASST models compare well with the Flightlab model and the Bell model 301 mathematical model.

Table 2: Comparison of eigenvalues of XV-15 model.

	Helicopter Mode $\beta_i = 90°$, Hover $\delta_f = 40°$	Helicopter Mode $\beta_i = 90°$, 120 kts $\delta_f = 40°$	Conversion Mode $\beta_i = 60°$, 120 kts $\delta_f = 40°$	Conversion Mode $\beta_i = 30°$, 140 kts $\delta_f = 40°$	Airplane Mode $\beta_i = 0°$, 260 kts $\delta_f = 0°$
Short period	-0.65, -0.218 [a, b] -0.68, 0.143 [c] -1.32, -0.105 [e]	-1.07 $\pm$ 2.61j [a] -1.19 $\pm$ 2.65j [b] -1.41 $\pm$ 2.79j [c] -1.44 $\pm$ 2.98j [d]	-1.27 $\pm$ 1.153j [a] -1.31 $\pm$ 1.855j [b] -1.29 $\pm$ 2.5j [c] -1.31 $\pm$ 2.539j [d]	-1.17 $\pm$ 1.41j [a] -1.28 $\pm$ 1.98j [b] -1.26 $\pm$ 2.29j [d]	-2.01 $\pm$ 2.73j [a] -1.97 $\pm$ 2.65j [b] -2.20 $\pm$ 4.59j [c] -2.24 $\pm$ 3.54j [d]
Longitudinal Phugoid	0.14 $\pm$ 0.39j [a, b] 0.15 $\pm$ 0.42j [c] 0.268 $\pm$ 0.513j [e]	-0.092 $\pm$ 0.022j [a] -0.083 $\pm$ 0.096j [b] -0.054 $\pm$ 0.076j [c] -0.034 $\pm$ 0.12j [d]	-0.082 $\pm$ 0.261j [a] -0.099 $\pm$ 0.248j [b] -0.077 $\pm$ 0.173j [c] -0.073 $\pm$ 0.261j [d]	-0.062 $\pm$ 0.245j [a] -0.2025 $\pm$ 0.261j [b] -0.136 $\pm$ 0.283j [d]	-0.021 $\pm$ 0.114j [a] -0.2 $\pm$ 0.207j [b] -0.17 $\pm$ 0.17j [c] -0.012 $\pm$ 0.139j [d]
Dutch roll	0.040 $\pm$ 0.21j [a, b] 0.006 $\pm$ 0.31j [c] 0.18 $\pm$ 0.406j [e]	-0.15 $\pm$ 1.01j [a, b] -0.24 $\pm$ 1.34j [c] -0.31 $\pm$ 1.33j [d]	-0.145 $\pm$ 1.16j [a, b] -0.215 $\pm$ 1.41j [c] -0.204 $\pm$ 1.52j [d]	-0.245 $\pm$ 1.122j [a, b] -0.198 $\pm$ 1.583j [d]	-0.511 $\pm$ 2.159j [a] -0.509 $\pm$ 2.56j [b] -0.63 $\pm$ 2.82j [c] -0.492 $\pm$ 2.36j [d]
Spiral	-0.061 [a, b] 0.136 [c] -0.102 [e]	-0.031 [a, b] -0.048 [c] -0.043 [d]	-0.074 [a, b] -0.06 [c] -0.042 [d]	-0.15 [a, b] -0.11 [d]	-0.083 [a, b] -0.075 [c] -0.071 [d]
Roll subsidence	-0.792 [a, b] -0.732 [c] -1.23 [e]	-1.59 [a, b] -1.37 [c] -1.67 [d]	-1.89 [a, b] -1.63[c] -1.64 [d]	-1.76 [a, b] -1.59 [d]	-1.54 [a] -1.52 [b] -1.41 [c] -1.75 [d]

[a] MASST model with engine dynamics with governor
[b] MASST model without engine dynamics
[c] Flightlab model[16]
[d] Bell Model 301 mathematical model[17]
[e] Identified model from flight test data[18]

In conversion and airplane mode, all the eigenmodes have comparable frequencies except for longitudinal phugoid mode. As mentioned earlier in section 2.3, the addition of engine and governor dynamics to XV-15's mathematical model reduces the damping of longitudinal phugoid mode in conversion and airplane mode. The MASST model without engine dynamics and Flightlab model have comparable eigenvalues and higher phugoid mode damping, as both models assume an ideal rotor with constant angular speed. On the other hand, MASST model with engine-governor dynamics and Bell model 301 mathematical model have comparable phugoid eigenvalues with lower damping.

3. quasi-LINEAR PARAMETER VARYING (qLPV) FLIGHT DYNAMICS MODEL

3.1. Theory

Linear state-space models that vary continuously with time varying scheduling parameters $\rho(t)$ are known as Linear Parameter Varying (LPV). The linear state-space models and the corresponding trim states and controls, obtained at the discrete trim points, are interpolated as function of the scheduling parameters. The definition of LPV model is[5]:

$$\dot{\mathbf{x}}(t) = \mathbf{A}(\boldsymbol{\rho}(t))\,\mathbf{x}(t) + \mathbf{B}(\boldsymbol{\rho}(t))\,\mathbf{u}(t) \tag{2}$$

If a subset of scheduling parameters is also state of the system, the model is called quasi-LPV (qLPV). Consider a state vector $\mathbf{x}(t)$ that is composed of scheduling states $\mathbf{z}(t)$ and non-scheduling states $\mathbf{w}(t)$, then the qLPV model is defined as:

$$\begin{bmatrix} \dot{\mathbf{z}}(t) \\ \dot{\mathbf{w}}(t) \end{bmatrix} = \mathbf{A}(\boldsymbol{\rho}(t)) \begin{bmatrix} \mathbf{z}(t) \\ \mathbf{w}(t) \end{bmatrix} + \mathbf{B}(\boldsymbol{\rho}(t))\,\mathbf{u}(t) \tag{3}$$

Scheduling parameter vector is composed of scheduling states and exogenous scheduling variables i.e., $\boldsymbol{\rho}(t) = [\,\mathbf{z}(t) \quad \boldsymbol{\xi}(t)\,]$.

To improve the quality of the model, the model stitching technique was proposed by Tischler[4], where the qLPV model is combined with rigid body nonlinear equations of motion and nonlinear gravitational force equations to obtain a continuous flight dynamics *stitched* model that is valid for the entire flight envelope.

3.2. XV-15 qLPV Model

The two key components of a quasi-Linear Parameter Varying *stitched* model are the lookup tables of discrete linear state-space models and the rigid body nonlinear equations of motion combined with the nonlinear gravitational forces. The qLPV model for XV-15 is developed by scheduling the linear state-space models with a four dimensional scheduling parameter $\boldsymbol{\rho}(t) = \begin{bmatrix} h & \beta_i & \delta_f & V \end{bmatrix}$. The model structure of qLPV model for XV- 15 is shown in Figure 6. The scheduling parameters h and V, are dependent upon the states of the system ($V = \sqrt{u^2 + w^2}$ and $\dot{h} = u \sin\theta - w \cos\theta$). This endogenous dependency of scheduling parameter vector on the state of the system may result in a nonlinear feedback through the state-space matrices and is referred to as quasi-LPV.

Firstly, the states and the corresponding linear state-space matrices are decomposed into six degrees-of-freedom rigid body states and higher order states. These discrete linear state-space models (trim states, trim control inputs and linear state-space matrices) obtained by MASST are subsequently interpolated as function of scheduling parameter vector $\boldsymbol{\rho}(t) = \begin{bmatrix} h & \beta_i & \delta_f & V \end{bmatrix}$. The interpolated trim states and control inputs are then subtracted from the current states and control inputs to obtain perturbation in states and control inputs, such that,:

$$\begin{aligned} \Delta\mathbf{x} &= \mathbf{x} - \mathbf{x}_{trim}(\boldsymbol{\rho}(t)) \\ \Delta\mathbf{u} &= \mathbf{u} - \mathbf{u}_{trim}(\boldsymbol{\rho}(t)) \end{aligned} \tag{4}$$

if the simulation starts at one of the discrete trimmed operating points, then these perturbations are zero. These perturbations are then multiplied with the interpolated linear state-space matrices. Multiplication of these perturbations with rigid body stability and control derivatives and mass matrix result in perturbed aerodynamic forces and moments. Furthermore, multiplication of state and control perturbations with higher order state-space matrices provide higher order state accelerations. The perturbed aerodynamic forces and moments are combined with the nonlinear gravitational forces and are used to obtain the rigid body state derivatives through nonlinear equations of motion. Rigid body state derivatives along with higher order state derivatives are integrated to obtain the current states. Three of the states u, w, θ, are used to obtain the current value of scheduling parameters velocity V and altitude h, as mentioned earlier.

It should be noted that filtered velocity $V_{filtered}$ with cutoff frequency $\omega_f = 0.2 rad/s$ is used to interpolate the stability and control derivatives to retain accurate dynamic response at the discrete operating points by ensuring constant derivative values for short term motion. It is also important to mention here that the Coriolis terms ($Z_q = Z_q - u_{trim}\, q$ etc.) and linearized gravity terms are removed form the state matrix $\mathbf{A}(\rho(t))$ of the MASST model since they are added as nonlinear terms in the equations of motion and gravitational force equations, respectively. Lastly, control derivatives associated with wing flap δ_f are set to zero as δ_f is one of the scheduling parameters and the effect of wing flap is preserved implicitly in the model by the variation in trim states and controls.

3.3. Actuator Dynamics

A first order actuator dynamic model, Eq. 5, is implemented. Time constants for actuators and corresponding saturation limits[19] are presented in Table 3.

$$G_{act}(s) = \frac{1}{\tau_{act} s + 1} \tag{5}$$

Furthermore, two different constant nacelle angle conversion rates are considered i.e., $\dot{\beta} = 3$ deg/s for nacelle angles greater than 75° and $\dot{\beta} = 8$ deg/s for nacelle angles less than 75°.

3.4. Stability and Control Augmentation System (SCAS)

To achieve level 1 handling qualities, SCAS system is adapted from Ref[17,20] and is integrated with the qLPV model of XV-15. The SCAS commands for pitch and roll axes come from rate feedback to augment the aircraft damping, attitude feedback for attitude retention and pilot stick input feed forward. For yaw axis, the SCAS command comes only as a combination of rate feedback and pilot pedal input feedforward.

3.5. Time Response Analysis

qLPV *stitched* model of XV-15 is validated by comparing SCAS off time responses with the time responses presented in the existing literature. As an example, Figures 7-9 show the time histories of pitch rate q and pitch angle θ, when a longitudinal stick input is applied to XV-15 in helicopter mode, airplane mode and conversion mode with $\beta_i = 60^\circ$. Figures 7-8 show the comparison of time histories with NASA'S generic tilt-rotor simulation (GTRS) model[21]. Figure 9 shows the comparison of time histories in conversion mode with flightlab model of

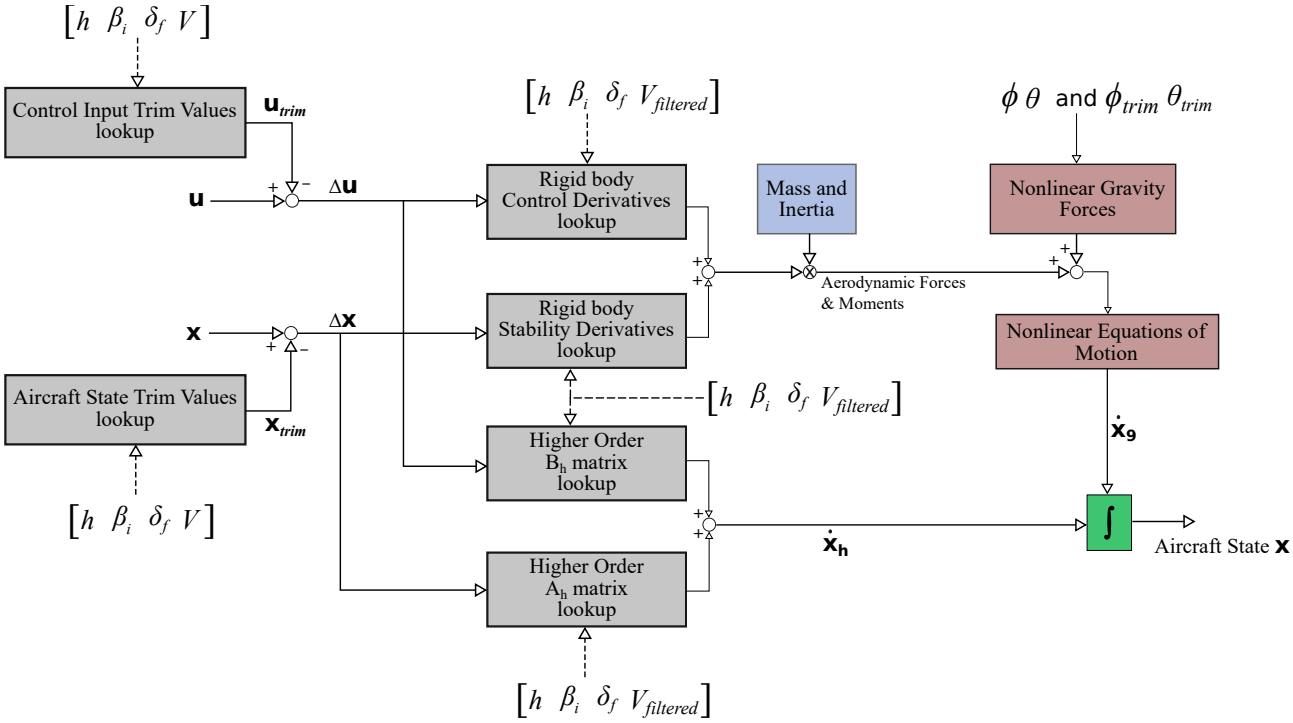

Figure 6: qLPV *stitched* model structure for XV-15 (adapted from Ref.[4]).

Table 3: Actuator time constant and saturation limits.

Actuator Type	Control	Time Constant τ_{act} [s]	Saturation Limit [deg.]	Positive Deflection
Rotor Controls	Collective θ_0	0.040	[-5 49]	Up
	Longitudinal cyclic θ_{1s}		[-10 10]	Forward
	Lateral cyclic θ_{1c}		[-10 10]	Right
Aerodynamic Surfaces	Flap δ_f	0.500	[0 75]	Trailing edge down
	Elevator δ_e		[-20 20]	Trailing edge down
	Aileron δ_a	0.077	[-13.8 23.8]	Right trailing edge down
	Rudder δ_r		[-20 20]	Right

XV-15[16]. A reasonable comparison and agreement is observed between qLPV model and GTRS and FXV-15 (Flightlab XV-15) model. Gearing ratio for longitudinal stick to elevator $\frac{\partial \delta_e}{\partial X_{col}} = 4.735$ deg/in is used instead of 4.16 deg/in (original value used in GTRS and Flightlab model), and hence the slight difference in the longitudinal responses of qLPV model and GTRS and flightlab model of XV-15.

4. REAL TIME FLIGHT SIMULATION

The design of rotorcraft is a difficult task that requires to take into account numerous, often conflicting constraints and requirements. During the early phases of the conceptual and preliminary design phases of a novel machine, the natural tendency of a designer is to take decisions based on a limited set of objectives using personal and company experience to guide the process. This approach can lead often to non-optimal machine, and in some cases to problems that are often highlighted only during the flight test phase with large associated costs for the required fixes[22]. This problem may be particularly important when new disruptive configurations are designed. To take into account the design aspects related to flight and handling qualities of the aircraft to be designed, it is necessary to give a pilot the possibility to test the capability of the aircraft. In fact, the most natural way to assess the performance of a design-stage virtual prototype is through pilot-in-the-loop flight simulation. Additionally, this type of simulation could be performed to support the certification process of a new aircraft.

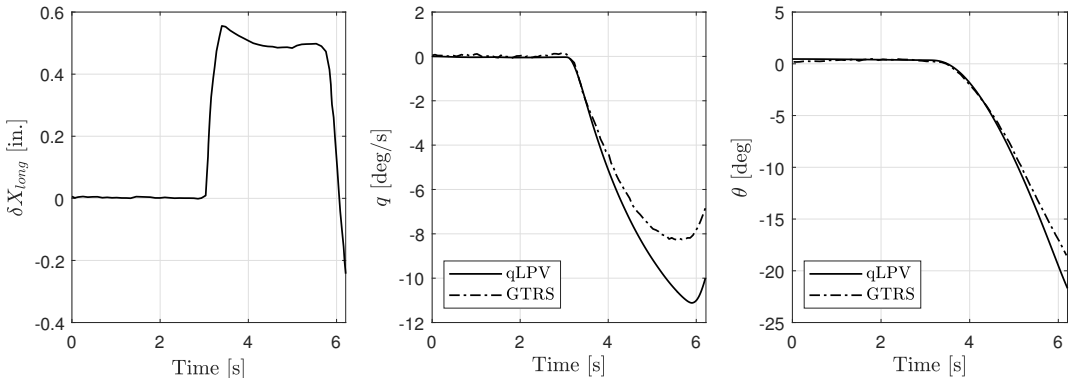

Figure 7: Time history correlation of SCAS OFF pitch response in helicopter mode at 0 kts.

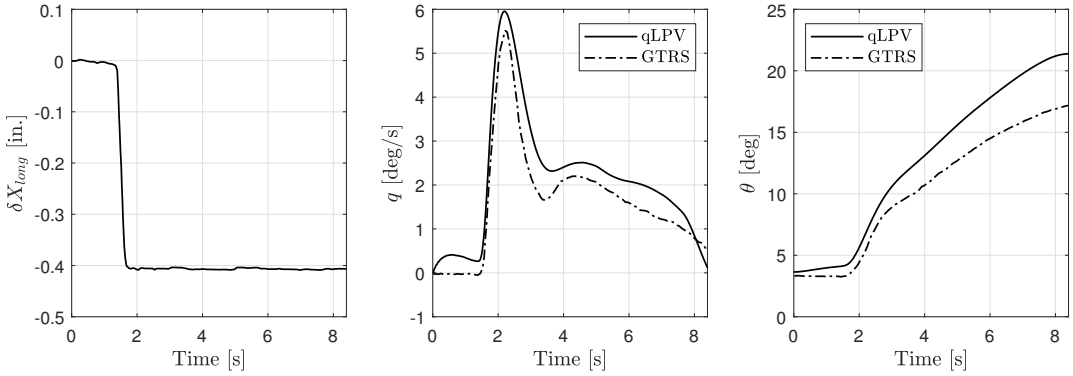

Figure 8: Time history correlation of SCAS OFF pitch response in airplane Mode at 175 kts.

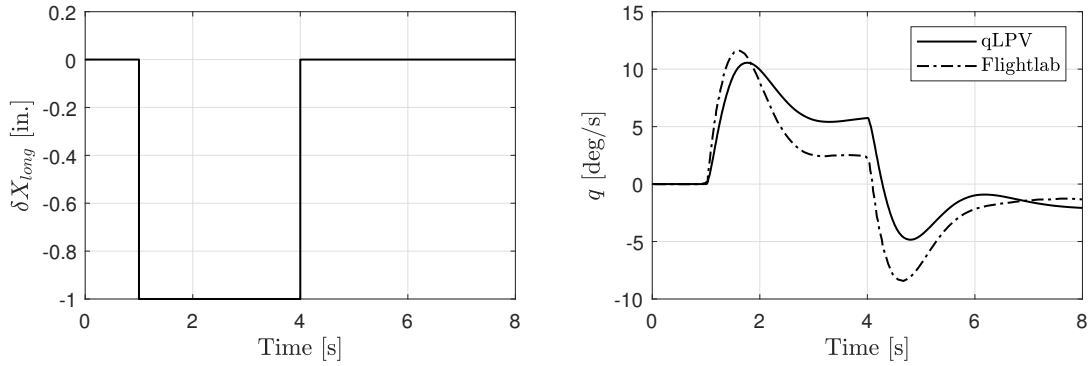

Figure 9: Time history correlation of SCAS OFF pitch response in conversion mode ($\beta_i = 60^0$) at 120 kts.

4.1. FRAME-SIM Flight Simulator

The FRAME-Sim rotorcraft flight simulation system, currently under development at the Department of Aerospace Science and Technology, Politecnico di Milano, was developed with these objectives in mind[23,24]. Consequently, a low-cost COTS-based flight simulator with the capability to be easily customized and modified, both from the hardware and the software point of view has been developed.

A fixed-base setup is chosen for the simulator hardware. Since the focus of the research activity will be given to flight quality prediction of new rotorcraft designs and the users are expected to be highly trained test pilots, motion feedback was deemed unnecessary.

The hardware is composed of the following elements:

1. **Visual system**: composed of a spherical projection screen and two HD-projectors, whose

emitted light is reflected onto two spherical mirrors to cover the full screen area.

2. **Glass cockpit**: comprises of two 20″ touchscreen LCD monitors and up to four 20″ standard (non-touchscreen) LCD monitors that display non-interactive flight instruments.

3. **Control inceptors**: to which force feedback is provided through four brushless motors, that are also responsible for the controls position sensing.

In addition, it is possible to substitute the visual system and the glass cockpit with a Virtual Reality (VR) headset. The use of Virtual Reality (VR) headsets are subject of increasing interest in flight simulation research for their potential in offering access to highly immersive environments in a cost-effective way. Details on this configuration can be found in Daniele et al.[25].

The FRAME-Sim software is composed of several modules:

1. **Flight dynamics module**: a multibody model of the aircraft is simulated exploiting the real-time capabilities of MBDyn, a multibody software. In the current research, flight dynamics module is based on qLPV *stitched* model and is implemented in Matlab®/Simulink®.

2. **Visual cueing module**: the free, open source software FlightGear is used to visualize the environment.

3. **Flight control system**: both MBDyn-based and Matlab®/Simulink®-based Flight Control System (FCS) models can be integrated in the simulation.

4. **Control inceptors input**: depending on the specific requirements of the simulation task, either the input from the brushless motors' encoder or joystick input through Human Interface Device (HID) module can be employed.

4.2. Real-Time Implementation of qLPV model

qLPV *stitched* model of XV-15 along with the actuator dynamics and stability and contorl augmentation system is implemented in Matlab®/Simulink®. Simulation parameters are listed in Table 4. In order to shorten the run time, simulation was run in *accelerator mode* of Simulink®.

Table 4: Simulation Parameters.

Integration type	Fixed step
Step size	0.003 s
Solver	ode4 (Runge-Kutta)

4.2.1. Lookup Tables Implementation

The qLPV model architecture require linear state-space models and the trim data to be formatted as a regular rectangular grid. Rectangular grid is generated by *clipping* and keeping the edge models, where state-space models and corresponding trim data are not available (e.g., High speeds at high nacelle incidence angles and low speeds at low nacelle incidence angles). This resulted in 1160 linear state-space models.

Trim states and controls are linearly interpolated using the *Prelookup* and *Interpolation using Prelookup* blocks. State and control matrices are interpolated linearly in the same manner, however, instead of interpolating each element of $\mathbf{A}$ and $\mathbf{B}$ matrices, only those elements are interpolated that show notable variation with scheduling parameters.

5. CONCLUSIONS

This paper presented the development of a high order quasi-Linear Parameter Varying (qLPV) *stitched* model for XV-15 for the purpose of real-time piloted simulation. The linear state-space models and the corresponding trim data are scheduled using four dimensional lookup tables: altitude, nacelle angle, wing flap deflection and aircraft velocity. Additional modules of actuator dynamics and stability and control augmentation system (SCAS) are also incorporated in the qLPV based flight dynamics model.

A proportional-integral (PI) based rotor speed governor is implemented to maintain a constant rotor speed. The PI gains are scheduled with nacelle incidence angle and aircraft velocity.

The paper also presented the details of FRAME-Sim, a fixed base rotorcraft flight simulation system to simulate tiltrotors using the q-LPV model presented here.

In the future, research will focus on the effects of number of scheduling parameters and number of states on the computational efficiency of qLPV models. Moreover, multivariate simplex B-spline polynomials will be developed to accurately and efficiently interpolate between the linear state-space models and corresponding trim data. Future work will also extend to the development of robust nonlinear control synthesis for qLPV systems and effective control

allocation techniques for tiltrotor aircraft.

ACKNOWLEDGEMENTS

The NITROS (Network for Innovative Training on ROtorcraft Safety) project has received funding from the European Union's Horizon 2020 research and innovation program under the Marie Skłdowska-Curie grant agreement # 721920.

REFERENCES

[1] Leonardo Helicopters. Aw609 for search and rescue. In *Dubai Airshow*, November 2017. URL `https://www.slideshare.net/webfinmeccanica/aw609-for-search-and-rescue`.

[2] J. Renaud, H. Huber, and G. Venn. The eurofar program – an european overview on advanced vtol civil transportation system. In *17th European Rotorcraft Forum*, September 1991.

[3] Philippe Rollet. Rhilp – a major step for european knowledge in tilt-rotor aeromechanics and flight dynamics. *Air & Space Europe*, 3 (3-4):152–154, May–August 2001. doi: $10.1016/S1290\text{-}0958(01)90080\text{-}2$.

[4] Eric L. Tobias and Mark B. Tischler. A model stitching architecture for continuous full flight-envelope simulation for fixed-wing aircraft and rotorcraft from discrete-point linear models. U.S. Army AMRDEC SR RDMR–AF–16–01, 2016.

[5] Andrès Marcos and Gary J. Balas. Development of linear-parameter-varying models for aircraft. *Journal of Guidance, Control and Dynamics*, 27(2):218–228, March–April 2004. doi: $10.2514/1.9165$.

[6] Ben Lawrence, Carlos A. Malpica, and Colin R. Theodore. The development of a large civil tiltrotor simulation for hover and low-speed handling qualities investigations. In *36th European Rotorcraft Forum*, September 2010.

[7] Tom Berger, Ondrej Juhasz, Mark J. S. Lopez, Mark B. Tischler, and Joseph F. Horn. Modeling and control of lift offset coaxial and tiltrotor rotorcraft. In *44th European Rotorcraft Forum*, September 2018.

[8] Vincenzo Muscarello, Francesca Colombo, Giuseppe Quaranta, and Pierangelo Masarati. Aeroelastic rotorcraft–pilot couplings in tiltrotor aircraft. *Journal of Guidance, Control, and Dynamics*, 42(3):524–537, 2019.

[9] Hafiz Noor Nabi, Coen de Visser, Marilena D. Pavel, and Giuseppe Quaranta. A quasi-linear parameter varying (qlpv) approach for tiltrotor conversion modeling and control synthesis. In *American Helicopter Society 75th Annual Forum*, May 2019.

[10] Pierangelo Masarati, Vincenzo Muscarello, and Giuseppe Quaranta. Linearized aeroservoelastic analysis of rotor-wing aircraft. In *36th European Rotorcraft Forum*, September 2010.

[11] Francesca Colombo, Vincenzo Muscarello, Giuseppe Quaranta, and Pierangelo Masarati. A comprehensive aeroservoelastic approach to detect and prevent rotorcraft-pilot coupling phenomena in tiltrotors. In *American Helicopter Society 74th Annual Forum*, May 2018.

[12] Wayne Johnson. Camrad/ja, a comprehensive analytical model of rotorcraft aerodynamics and dynamics- volume i: Theory manual. Johnson Aeronautics Version, 1988.

[13] C. W. Acree. An improved camrad model for aeroelastic stability analysis of the xv-15 with advanced technology blades. NASA TM 4448, 1993.

[14] Dale M. Pitt and David A. Peters. Theoretical prediction of dynamic inflow derivatives. In *6th European Rotorcraft and Powered Lift Aircraft Forum*, September 1980.

[15] Joseph Schaeffer, Roger Alwang, and Mukung Joglekar. V-22 thrust power management control law development. In *American Helicopter Society 47th Annual Forum*, May 1991.

[16] Gareth D. Padfield. *Helicopter Flight Dynamics: Including a Treatment of Tiltrotor Aircraft*. John Wiley & Sons, West Sussex, UK, 2018.

[17] P. B. Harendra, M. J. Joglekar, T. M. Gaffey, and R. L. Marr. A mathematical model for real time flight simulation of the bell model 301 tilt rotor research aircraft. Bell Helicopter CR 114614, 1973.

[18] Mark B. Tischler. Frequency-response identification of xv-15 tilt-rotor aircraft dynamics. NASA TM 89428, 1987.

[19] Roger L. Marr, J. Marvin Willis, and Gary B. Churchill. Flight control system development for the xv-15 tilt rotor aircraft. In *American Helicopter Society 32nd Annual Forum*, May 1976.

[20] Samuel W. Ferguson. A mathematical model for real time flight simulation of a generic tiltrotor aircraft. NASA CR 166536, 1988.

[21] Samuel W. Ferguson. Development and validation of a simulation for a generic tilt-rotor aircraft. NASA CR 166537, 1989.

[22] Stephen J Kapurch. *NASA systems engineering handbook*. Diane Publishing, 2010.

[23] Andrea Zanoni, Luca Conti, and Pierangelo Masarati. Frame-sim: A free-software, multibody-based, pilot in the loop rotorcraft flight simulator. In *ASME 2018 International Design Engineering Technical Conferences and*

Computers and Information in Engineering Conference, pages 1–8, 2018.

[24] Andrea Zanoni, Pierangelo Masarati, and Giuseppe Quaranta. Physics-based piloted flight simulation of helicopters using multibody dynamics. In *ASME 2016 International Design Engineering Technical Conferences and Computers and Information in Engineering Conference*, 2016.

[25] Matteo Daniele, Andrea Zanoni, Pierangelo Masarati, and Giuseppe Quaranta. Development of a virtual reality real-time helicopter flight simulator. In *AIDAA XXV International Congress*, 2019.